Fine-Tuning of the Cytoplasmic Ca^{2+} Concentration Is Essential for Pollen Tube Growth[1][W]

Megumi Iwano*, Tetsuyuki Entani, Hiroshi Shiba, Mituru Kakita, Takeharu Nagai, Hideaki Mizuno, Atsushi Miyawaki, Tsubasa Shoji, Kenichi Kubo, Akira Isogai, and Seiji Takayama

Graduate School of Biological Sciences, Nara Institute of Science and Technology, Ikoma, Nara 630–0101, Japan (M.I., T.E., H.S., M.K., T.S., K.K., A.I., S.T.); Research Institute for Electronic Science, Hokkaido University, Sapporo, Hokkaido 060–0812, Japan (T.N.); and Brain Science Institute, The Institute of Physical and Chemical Research (RIKEN), Wako, Saitama 351–0198, Japan (H.M., A.M.)

Pollen tube growth is crucial for the delivery of sperm cells to the ovule during flowering plant reproduction. Previous in vitro imaging of *Lilium longiflorum* and *Nicotiana tabacum* has shown that growing pollen tubes exhibit a tip-focused Ca^{2+} concentration ([Ca^{2+}]) gradient and regular oscillations of the cytosolic [Ca^{2+}] ([Ca^{2+}]$_{cyt}$) in the tip region. Whether this [Ca^{2+}] gradient and/or [Ca^{2+}]$_{cyt}$ oscillations are present as the tube grows through the stigma (in vivo condition), however, is still not clear. We monitored [Ca^{2+}]$_{cyt}$ dynamics in pollen tubes under various conditions using Arabidopsis (*Arabidopsis thaliana*) and *N. tabacum* expressing yellow cameleon 3.60, a fluorescent calcium indicator with a large dynamic range. The tip-focused [Ca^{2+}]$_{cyt}$ gradient was always observed in growing pollen tubes. Regular oscillations of the [Ca^{2+}]$_{cyt}$, however, were rarely identified in Arabidopsis or *N. tabacum* pollen tubes grown under the in vivo condition or in those placed in germination medium just after they had grown through a style (semi-in vivo condition). On the other hand, regular oscillations were observed in vitro in both growing and nongrowing pollen tubes, although the oscillation amplitude was 5-fold greater in the nongrowing pollen tubes compared with growing pollen tubes. These results suggested that a submicromolar [Ca^{2+}]$_{cyt}$ in the tip region is essential for pollen tube growth, whereas a regular [Ca^{2+}] oscillation is not. Next, we monitored [Ca^{2+}] dynamics in the endoplasmic reticulum ([Ca^{2+}]$_{ER}$) in relation to Arabidopsis pollen tube growth using yellow cameleon 4.60, which has a lower affinity for Ca^{2+} compared with yellow cameleon 3.60. The [Ca^{2+}]$_{ER}$ in pollen tubes grown under the semi-in vivo condition was between 100 and 500 μM. In addition, cyclopiazonic acid, an inhibitor of ER-type Ca^{2+}-ATPases, inhibited growth and decreased the [Ca^{2+}]$_{ER}$. Our observations suggest that the ER serves as one of the Ca^{2+} stores in the pollen tube and cyclopiazonic acid-sensitive Ca^{2+}-ATPases in the ER are required for pollen tube growth.

In many flowering plants, a pollen grain that lands on the top surface of a stigma will hydrate and germinate a pollen tube. Following germination, the pollen tube enters the style and grows through the wall of transmitting tract cells on the way to the ovary, where the tube emerges to release the sperm for double fertilization. Therefore, pollen tube growth is essential for reproduction in flowering plants.

Since Brewbaker and Kwack (1963) revealed that Ca^{2+} is essential for in vitro pollen tube cultures, the relationship between the Ca^{2+} concentration ([Ca^{2+}]) and pollen tube growth has been further examined under in vitro germination culture conditions. Ratiometric ion imaging using fluorescent dye has revealed that the apical domain of a pollen tube grown in vitro contains a tip-focused [Ca^{2+}] gradient (Pierson et al., 1994, 1996; Cheung and Wu, 2008) and that the cytoplasmic [Ca^{2+}] ([Ca^{2+}]$_{cyt}$) in the tip region and the growth rate oscillate with the same periodicity (Pierson et al., 1996; Holdaway-Clarke et al., 1997; Messerli and Robinson, 1997). Therefore, oscillation of the [Ca^{2+}]$_{cyt}$ has been thought to correlate with pollen tube growth. It is not clear, however, whether regular [Ca^{2+}]$_{cyt}$ oscillations in the tip region occur in pollen tubes growing through stigmas and styles.

The [Ca^{2+}]$_{cyt}$ is controlled temporally and spatially by transporters in the membranes of intracellular compartments and in the plasma membrane (Sze et al., 2000). Studies using a Ca^{2+}-sensitive vibrating electrode revealed Ca^{2+} influx in the tip region of the pollen tube (Pierson et al., 1994; Holdaway-Clarke et al., 1997; Franklin-Tong et al., 2002). Stretch-activated Ca^{2+} channels have been found in the plasma membrane using patch-clamp electrophysiology (Kuhtreiber and Jaffe, 1990; Dutta and Robinson, 2004). Recently, CNGC18 was identified as a Ca^{2+}-permeable channel in the plasma membrane that is essential for pollen tube growth (Frietsch et al., 2007). The intracellular compart-
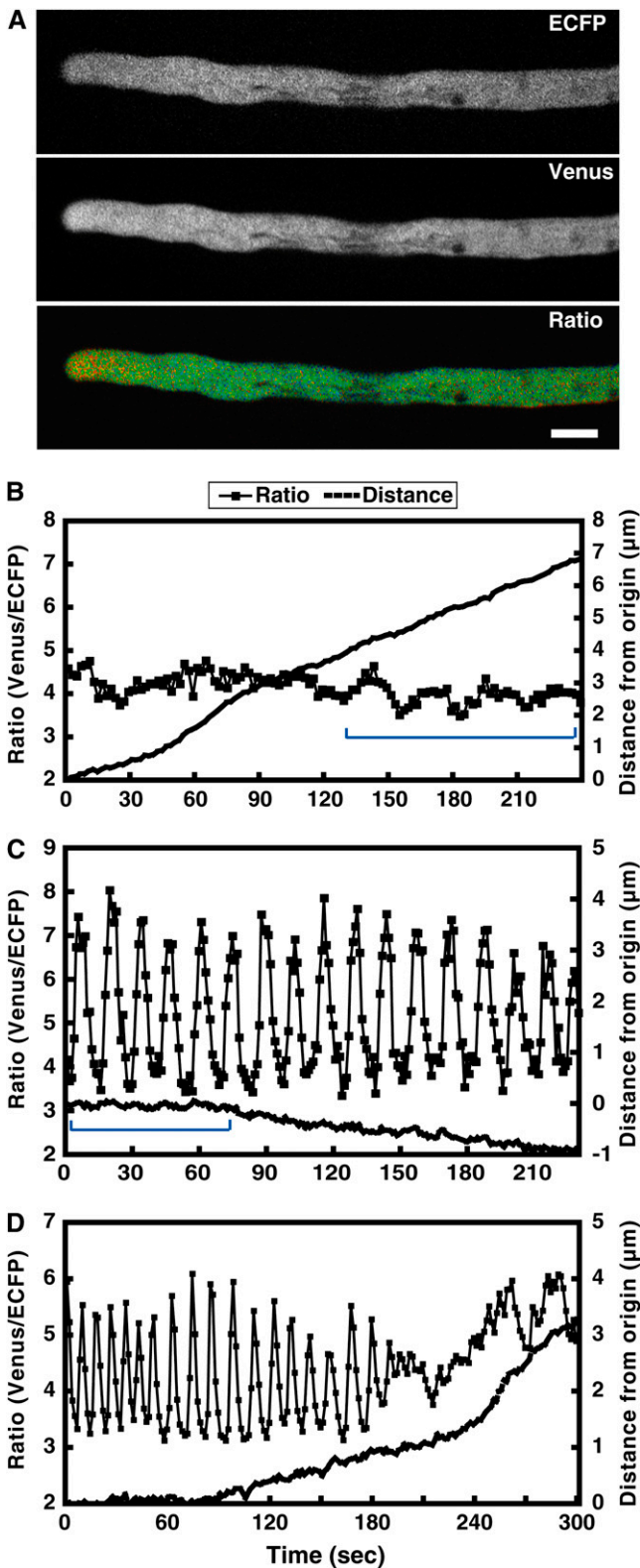
Figure 1. Irregular and regular $[Ca^{2+}]_{cyt}$ oscillations observed in elongated Arabidopsis pollen tubes 5 h after dissemination under the in vitro condition. A, ECFP, Venus, and ratio (Venus/ECFP) images of an elongated pollen tube 5 h after dissemination. A tip-focused $[Ca^{2+}]_{cyt}$ gradient was observed. The ratio (Venus/ECFP) in a tip area with a

ments that store Ca^{2+} in the pollen tube and the relevant Ca^{2+} transporters, however, have yet to be identified.

Yellow cameleons are genetically encoded Ca^{2+} indicators that were developed to monitor the $[Ca^{2+}]$ in living cells (Miyawaki et al., 1997). These indicators are chimeric proteins consisting of enhanced cyan fluorescent protein (ECFP), calmodulin (CaM), a glycylglycine linker, the CaM-binding domain of myosin light chain kinase (M13), and enhanced yellow fluorescent protein (EYFP). When the CaM domain binds Ca^{2+}, the domain associates with the M13 peptide and induces fluorescence resonance energy transfer (FRET) between ECFP and EYFP. Several types of cameleons have been developed by tuning the CaM domain binding affinity for Ca^{2+}. Yellow cameleon 2.1 (YC2.1) is a high-affinity indicator that has been used to monitor the $[Ca^{2+}]_{cyt}$ in Arabidopsis (*Arabidopsis thaliana*) guard cells (Allen et al., 1999, 2000, 2001), *Lilium longiflorum* and *Nicotiana tabacum* pollen tubes (Watahiki et al., 2004), and the root hair of *Medicago truncatula* (Miwa et al., 2006). YC3.1 is a low-affinity indicator that has been used to monitor the $[Ca^{2+}]_{cyt}$ during pollen germination and in papilla cells of Arabidopsis (Iwano et al., 2004).

Recently, YC3.60 was developed as a new YC variant (Nagai et al., 2004), in which the acceptor fluorophore is a circularly permuted version of Venus rather than EYFP (Nagai et al., 2002). YC3.60 has a monophasic Ca^{2+} dependency with a dissociation constant (K_d) of 0.25 μM. Compared with YC3.1, YC3.60 is equally bright with a 5- to 6-fold larger dynamic range. Thus, YC3.60 results in a markedly enhanced signal-to-noise ratio, thereby enabling Ca^{2+} imaging experiments that were not possible with conventional YCs. On the other hand, YC4.60 was developed by mutating the Ca^{2+}-binding loop of CaM in YC3.60. Because YC4.60 has a significantly lower Ca^{2+} affinity with a biphasic Ca^{2+} dependency (K_d: 58 nM and 14.4 μM), it allows changes in $[Ca^{2+}]$ dynamics to be detected against a high background $[Ca^{2+}]$ (Nagai et al., 2004).

To examine whether the $[Ca^{2+}]_{cyt}$ oscillates in pollen tubes growing through a stigma after pollination (in vivo condition), in those placed in germination medium immediately after passing through a style (semi-in vivo condition), or in those grown in germination medium (in vitro condition), we generated transgenic Arabidopsis and *N. tabacum* lines expressing the *YC3.60*

diameter of 6 μm was measured. Bar = 10 μm. B, The ratio change in the tip region and the elongation of a normally growing pollen tube. Primarily irregular oscillations were observed, although relatively regular oscillations also were identified in the range marked with a blue line. C, The ratio change in the tip region of a relatively slowly growing pollen tube (blue line) and the distance moved during monitoring. Regular $[Ca^{2+}]_{cyt}$ oscillations with a large amplitude were observed. D, Regular oscillations followed by irregular oscillations. Regular oscillations were detected in a stopped or slowly growing pollen tube, whereas irregular oscillations were observed in a growing pollen tube.

gene in their pollen grains and monitored Ca^{2+} dynamics in the pollen tube tip. We also examined how inhibitors of pollen tube growth affect Ca^{2+} dynamics in pollen tubes growing under the semi-in vivo condition. To examine Ca^{2+} dynamics in the endoplasmic reticulum (ER), we generated transgenic Arabidopsis plants expressing YC4.60 in the pollen tube ER. The results are discussed in relation to the physiological relevance of $[Ca^{2+}]$ oscillations for pollen tube growth.

RESULTS

Expression of YC3.60 in Pollen Grains

Pollen grains harvested from Arabidopsis and *N. tabacum* plants transformed with *YC3.60* were transferred onto solid germination medium. Pollen tubes growing on the germination medium were observed using a fluorescence microscope (blue excitation), which allowed us to select plants with the brightest fluorescence signals. To confirm that the pollen tubes expressed the ECFP and Venus components of YC3.60, we obtained fluorescence spectra from the growing pollen tubes using a spectral-imaging microscope system with excitation at 458 nm. The YC3.60 spectrum was a combination of the spectra typically observed for recombinant ECFP and Venus proteins. Photobleaching a 5- $\times$ 10-μm area of the pollen tube tip with a 514-nm light induced an approximately 90% increase in ECFP fluorescence, which was higher than the 15% observed for YC3.1 (data not shown). These results demonstrated that full-length YC3.60 was expressed in the transgenic pollen tubes and that the FRET efficiency within YC3.60 was higher than that within YC3.1.

Ca^{2+} Imaging in Arabidopsis Pollen Tubes Grown in Vitro

First, we examined Arabidopsis pollen tubes grown in vitro for regular $[Ca^{2+}]_{cyt}$ oscillations, as has been observed in *L. longiflorum* and *N. tabacum*. Pollen grains from freshly dehisced anthers of YC3.60-expressing plants were mounted on germination medium. After 5 h, approximately 20% of the pollen grains germinated

with elongated pollen tubes. We continued to monitor pollen tubes that were at least 200 μm in length. The signals from ECFP and Venus (FRET image) at the tip of the pollen tubes were obtained at 50-ms to 5.0-s intervals with excitation at 440 nm; Venus/ECFP ratios were calculated from these images (Fig. 1A). ECFP and Venus fluorescence intensities in a tip region with a diameter of 6 μm were measured, and the Venus/ECFP ratio was calculated. $[Ca^{2+}]_{cyt}$ gradients were evident in pollen tubes that grew normally (growth rate: 2.0 $\pm$ 1.8 μm/min; Fig. 1A). Although some oscillations were observed (Fig. 1B), consistently regular $[Ca^{2+}]_{cyt}$ oscillations were not detected. The mean value of the maximum ratio was 4.5 $\pm$ 0.2, whereas the mean value of the minimum ratio was 3.9 $\pm$ 0.3 (Fig. 1B; Table I; Supplemental Video S1). The mean amplitude range was 0.3 $\pm$ 0.2, and the periodicity of the $[Ca^{2+}]_{cyt}$ oscillations was irregular, ranging from 4 to 30 s (Fig. 1B). These irregular $[Ca^{2+}]_{cyt}$ oscillations were observed in 45 of 55 pollen tubes observed under the in vitro condition. Four pollen tube tips burst during monitoring.

To convert the YC3.60 ratios into approximate $[Ca^{2+}]_{cyt}$ values, calibration of the $[Ca^{2+}]_{cyt}$ was carried out as described previously (Allen et al., 1999). Serial dilutions of purified YC3.60 protein were made in Ca^{2+} calibration buffer (Molecular Probes), in which the free $[Ca^{2+}]$ ranged from 0 μM to 1 mM. YC3.60 dilutions that resulted in signal intensities similar to those observed in YC3.60-expressing pollen tubes were used to determine minimum ratio (R_{min}) and maximum ratio (R_{max}). The obtained R_{min} and R_{max} values for YC3.60 were 2.95 and 8.33, respectively. These values were used to convert the YC3.60 fluorescence ratios into $[Ca^{2+}]_{cyt}$ by fitting them to YC3.60 titration curves obtained in vitro (Fig. 2A). In this way, we estimated that the $[Ca^{2+}]_{cyt}$ in the tip region shown in Figure 1B ranged from 0.3 to 0.4 μM.

On the other hand, regular $[Ca^{2+}]_{cyt}$ oscillations were also observed (Fig. 1C; Supplemental Video S2). These regular $[Ca^{2+}]_{cyt}$ oscillations were observed in five of 55 pollen tubes observed under the in vitro condition. In these cases, however, the pollen tube was not growing (Fig. 1C, blue line). The mean value of the maximum ratio was 7.2 $\pm$ 0.5, whereas the mean value of the

Table I. *$[Ca^{2+}]$ oscillation and growth rate of the pollen tube in Arabidopsis and N. tabacum*

Condition	Growth Rate	Max/Min Ratio	Amplitude Range	$[Ca^{2+}]_{cyt}$	Exp. No.
	μm/min			μM	
Arabidopsis					
In vitro	2.0 $\pm$ 1.8	4.5 $\pm$ 0.2/3.9 $\pm$ 0.3	0.3 $\pm$ 0.2	0.3–0.4	45
In vitro	<1.0	7.2 $\pm$ 0.5/3.5 $\pm$ 0.2	1.8 $\pm$ 0.3	0.3–1.0	5
In vivo	3.6 $\pm$ 0.5	4.0 $\pm$ 0.4/3.4 $\pm$ 0.3	0.4 $\pm$ 0.3	0.3–0.4	10
Semi-in vivo	3.1 $\pm$ 0.8	5.1 $\pm$ 0.5/4.5 $\pm$ 0.5	0.3 $\pm$ 0.2	0.4–0.5	48
N. tabacum					
In vitro	2.8 $\pm$ 1.6	3.9 $\pm$ 0.2/3.5 $\pm$ 0.2	0.2 $\pm$ 0.1	0.3–0.4	17
In vitro	<1.0	4.8 $\pm$ 0.4/2.8 $\pm$ 0.2	1.0 $\pm$ 0.1	0.1–0.5	5
In vivo	0.2 $\pm$ 0.1	3.5 $\pm$ 0.2/3.3 $\pm$ 0.1	0.1 $\pm$ 0.1	0.3	15
Semi-in vivo	1.2 $\pm$ 0.2	3.9 $\pm$ 0.4/3.4 $\pm$ 0.4	0.3 $\pm$ 0.2	0.3–0.4	30

Figure 2. Titration curves for YC3.60 and YC4.60.

growing through a stigma. Wild-type papilla cells were pollinated with YC3.60-expressing pollen grains. The pollen grains germinated within 20 min, and each pollen tube penetrated and elongated in a papilla cell wall within 30 min. The mean in vivo growth rate of the pollen tubes in the papilla cells was 3.6 ± 0.5 μm/min. Irregular $[Ca^{2+}]_{cyt}$ oscillations were observed in the tip regions of pollen tubes growing through the papilla cell walls 5 min after penetration (Fig. 3, A and B; Supplemental Video S4). The mean value of the maximum ratio was 4.0 ± 0.4, and the mean value of the minimum ratio was 3.4 ± 0.3 (Fig. 3B; Table I). The amplitude range of the ratio was 0.4 ± 0.3, which was significantly different ($P < 0.01$) from that of the regular $[Ca^{2+}]_{cyt}$ oscillations observed in vitro (Fig. 1C). In addition, compared with the $[Ca^{2+}]_{cyt}$ oscillations shown in Figure 1C, the periodicity of the $[Ca^{2+}]_{cyt}$ oscillations was more irregular. The data obtained in this experiment were not affected by the monitoring interval (data not shown). Irregular $[Ca^{2+}]_{cyt}$ oscillations were observed in all experiments under the in vivo condition (10/10 samples). In summary, regular $[Ca^{2+}]_{cyt}$ oscillations were not observed in pollen tubes as they grew through the papilla cell wall.

Ca²⁺ Imaging in Arabidopsis Pollen Tubes Growing under Semi-in Vivo Conditions

Arabidopsis pollen tubes were examined under the semi-in vivo condition after they grew through the pistil; this method facilitated the monitoring process because we were able to monitor a number of elongating pollen tubes simultaneously and the growth conditions better represented the in vivo condition (Iwano et al., 2004). We monitored the $[Ca^{2+}]_{cyt}$ in pollen tubes growing in the semi-in vivo condition at 50-ms to 2-s intervals. The mean growth rate was 3.1 ± 0.8 μm/min, and irregular $[Ca^{2+}]_{cyt}$ oscillations were in the pollen tube tips (Fig. 3, C and D; Supplemental Video S5). The mean values of the maximum and minimum ratios were 5.1 ± 0.5 and 4.5 ± 0.5, respectively, with an amplitude range of 0.3 ± 0.2 (Fig. 3D; Table I). Similar irregular $[Ca^{2+}]_{cyt}$ oscillations were observed in all experiments under the semi-in vivo condition (48/48 samples).

In order to confirm that the cameleon can technically detect $[Ca^{2+}]_{cyt}$ oscillations in semi-in vivo conditions, we obtained fluorescence spectra from the pollen tubes growing in the semi-in vivo condition in the presence of ionophore or in the presence of ionophore and EGTA using a spectral-imaging microscope system with excitation at 458 nm. Compared with that in the presence of ionophore alone (Fig. 4A), fluorescence of Venus component of YC3.60 was decreased in the presence of ionophore and EGTA, which is almost free from Ca²⁺ (Fig. 4B) Therefore, these results showed that Ca²⁺-dependent energy transfer from ECFP to Venus occurs also in the semi-in vivo condition.

minimum ratio was 3.5 ± 0.2 (Fig. 1C; Table I). The mean amplitude range was 1.8 ± 0.3, which was significantly different from that of the irregular $[Ca^{2+}]_{cyt}$ oscillations shown in Figure 1B. The $[Ca^{2+}]_{cyt}$ in the tip region was estimated to be between 0.1 and approximately 1 μM. The mean periodicity of the $[Ca^{2+}]_{cyt}$ oscillations was 13.8 ± 1.7 s. In addition, regular $[Ca^{2+}]_{cyt}$ oscillations followed by irregular oscillations were also observed in one sample (Fig. 1D; Supplemental Video S3). In this case, the length of the pollen tube was between 200 and 500 μm, and the regular $[Ca^{2+}]_{cyt}$ oscillations were observed only when the pollen tube stopped growing or grew slowly, whereas the irregular oscillations were observed in the normally growing pollen tube. These data suggested that regular $[Ca^{2+}]_{cyt}$ oscillations in the tip were not essential for Arabidopsis pollen tube growth in vitro.

Ca²⁺ Imaging in Arabidopsis Pollen Tubes Growing through Stigmas

To examine whether regular $[Ca^{2+}]_{cyt}$ oscillations occurred in vivo, we monitored the tips of pollen tubes

Figure 3. Irregular oscillations observed in Arabidopsis pollen tubes growing through a papilla cell wall (in vivo condition) and in pollen tubes growing through a style and then on germination medium (semi-in vivo condition). A, A ratio image of a pollen tube growing though a papilla cell obtained approximately 7.5 min after penetration. A tip-focused $[Ca^{2+}]$ gradient was observed. The papilla cell is marked with a white line. B, The ratio change in the tip of the pollen tube shown in A and the elongation of a pollen tube 5 min after penetration. The amplitude and period of the oscillations were irregular. C, Ratio images of a pollen tube that has just passed through the style. D, The ratio change in the tip of the pollen tube shown in C and elongation during monitoring. The amplitude and periodicity of the oscillations were irregular.
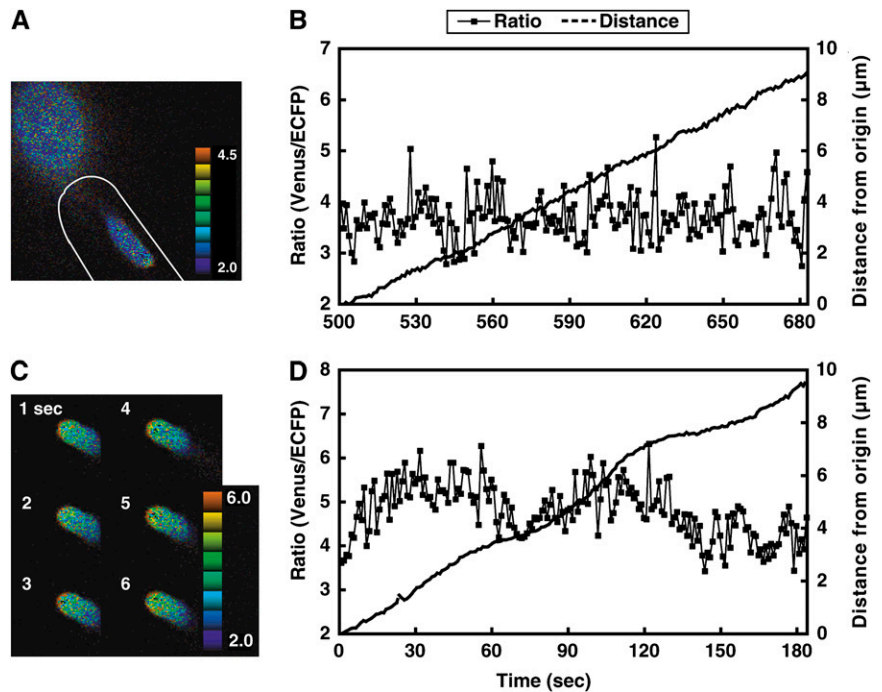

Effects of Pollen Tube Growth Inhibitors on Ca^{2+} Dynamics in Arabidopsis Pollen Tubes

We only observed regular $[Ca^{2+}]_{cyt}$ oscillations when the pollen tubes had stopped growing or when they grew slowly. We therefore speculated that regular $[Ca^{2+}]_{cyt}$ oscillations were directly related to arrest of pollen tube growth. It was previously shown that the growth rate and changes in the $[Ca^{2+}]_{cyt}$ were affected by Ca^{2+} channel blockers and chelators, such as Gd^{3+} and EGTA (Malhó et al., 1994; Geitmann and Cresti, 1998; Franklin-Tong et al., 2002). In addition, cyclopiazonic acid (CPA), a specific inhibitor of animal SERCA-type Ca^{2+}-ATPases (Inesi and Sagara, 1994) and plant

P-type IIA Ca^{2+}-ATPases (Geisler et al., 2000), affects the growth rate and $[Ca^{2+}]_{cyt}$ dynamics of pollen tubes.

First, we examined the effects of these inhibitors on pollen germination and the growth rate. Gd^{3+}, EGTA, and CPA arrested pollen tube growth in the semi-in vivo condition (Fig. 5). Next, we examined the effects of these inhibitors on $[Ca^{2+}]_{cyt}$ oscillations in pollen tubes growing in the semi-in vivo condition. The maximum $[Ca^{2+}]_{cyt}$ did not change, whereas the area with a high $[Ca^{2+}]_{cyt}$ increased in size just after the addition of CPA to the culture medium (final concentration: approximately 5 μM; Fig. 6). Regular $[Ca^{2+}]_{cyt}$ oscillations then were induced. These regular $[Ca^{2+}]_{cyt}$ oscillations were induced in five of 10 pollen tubes

Figure 4. The YC3.60 spectrum in the presence of ionophore (A) or in the presence of ionophore and EGTA (B).
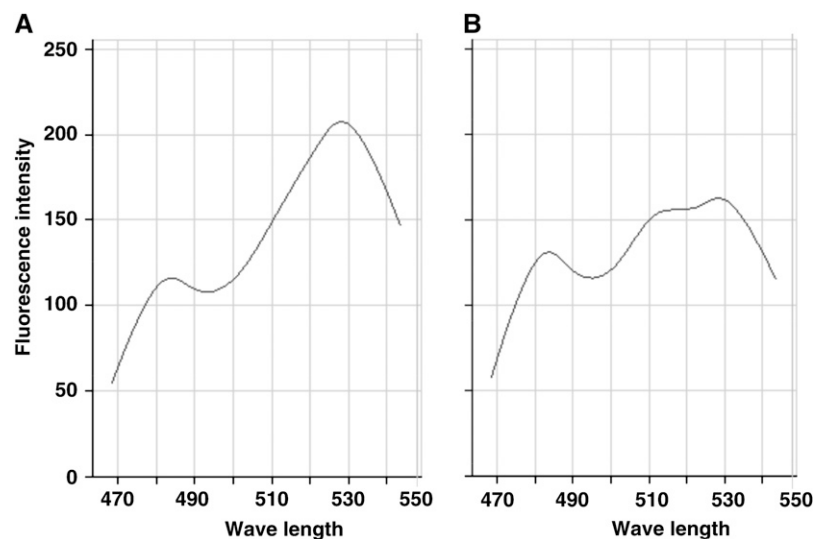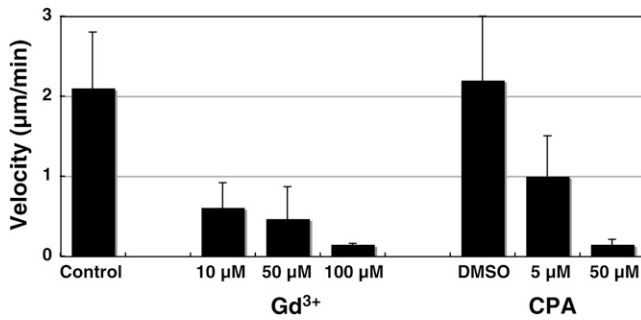
Figure 5. The effects of inhibitors on Arabidopsis pollen tube elongation. DMSO, Dimethyl sulfoxide.

treated with CPA. Two pollen tubes did not induce, and the other three burst during monitoring. After the addition of Gd^{3+} to these samples, the amplitude of the oscillations decreased and irregular oscillations were observed (Supplemental Video S6). On the other hand, application of Gd^{3+} alone arrested pollen tube growth but did not induce $[Ca^{2+}]_{cyt}$ oscillation at the tip (Fig. 7; Supplemental Video S7) yet caused a decrease of $[Ca^{2+}]_{cyt}$ at the tip, namely, the disappearance of a tip-focused $[Ca^{2+}]_{cyt}$ gradient (2 in Fig. 7A). Finally, many of the pollen tips burst, and the elevation of $[Ca^{2+}]_{cyt}$ over the whole area of pollen tube was caused by the influx of extracellular Ca^{2+} (3 in Fig. 7A). These results were repeatedly observed in 10 of 15 pollen tubes treated with Gd^{3+}. The other five burst before monitoring. These results showed that inhibitors of pollen tube growth induced abnormal $[Ca^{2+}]_{cyt}$ dynamics, including regular $[Ca^{2+}]_{cyt}$ oscillations and a disappearance of the tip-focused $[Ca^{2+}]_{cyt}$ gradient. Further-

more, these results suggested that the action site of Gd^{3+} is different from that of CPA and is related to the formation of the tip-focused $[Ca^{2+}]_{cyt}$ gradient.

Ca²⁺ Dynamics in the ER of Arabidopsis Pollen Tubes Growing in the Semi-in Vivo Condition

To confirm that ER functions as a Ca^{2+} store in the pollen tube, we monitored the $[Ca^{2+}]$ in the ER ($[Ca^{2+}]_{ER}$) of pollen tubes growing in the semi-in vivo condition and examined the effects of CPA treatment. We also generated transgenic Arabidopsis plants expressing a chimeric protein consisting of a signal peptide, YC4.60, and an ER retention signal. We monitored ECFP and Venus (FRET imaging) in a transgenic pollen tube passing through a pistil at 1- to 3-s intervals with excitation at 442 nm; the Venus/CFP fluorescence ratio was then calculated. Venus-labeled ER was localized longitudinally in the pollen tube (Fig. 8). Areas with a high $[Ca^{2+}]_{ER}$ were distributed sporadically throughout the pollen tube (Fig. 8; Supplemental Video S8) and no ER with a high $[Ca^{2+}]$ was observed in the tip of the growing pollen tube. The maximum ratio of the high $[Ca^{2+}]_{ER}$ areas was 9.5, which was estimated to correspond to between 100 and 500 μM (Fig. 2B).

When CPA was added to pollen tubes in the semi-in vivo condition (final concentration: approximately 5 μM), the ratio decreased in 2 min from approximately 9 to 5.5, which corresponds to between 0.1 and 1 μM, although pollen tube growth was not completely inhibited (Fig. 9). When additional CPA was added to the culture medium (final concentration: approximately 10 μM), the ratio decreased further and pollen tube growth was completely arrested. Similar decreases of the ratio by CPA were observed repeatedly
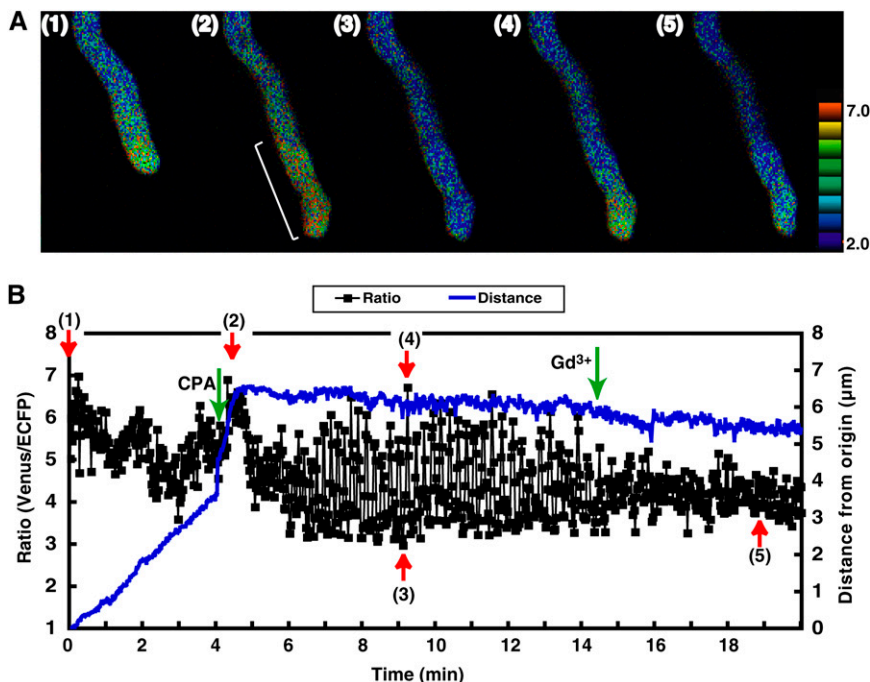

Figure 6. The effects of inhibitors on the changes in the $[Ca^{2+}]_{cyt}$ in the tip region of Arabidopsis pollen tubes growing in the semi-in vivo condition. A, Ratio images of a pollen tube. The numbers in each figure correspond to each point in the graph shown in B. After the addition of CPA, the $[Ca^{2+}]_{cyt}$ increased in a large area containing the tip region (white line). B, The ratio change in the tip region, an area from the pollen tube shown in A with a diameter of 6 μm. Blue line indicates distance from origin. Before the addition of CPA, irregular fluctuations were observed. Two minutes after the addition of CPA (shown with a green arrow), regular oscillations were induced. These oscillations were inhibited by the addition of Gd^{3+} (shown with a green arrow). Red arrows (1) to (5) correlate to the ratio images in Figure 6A.
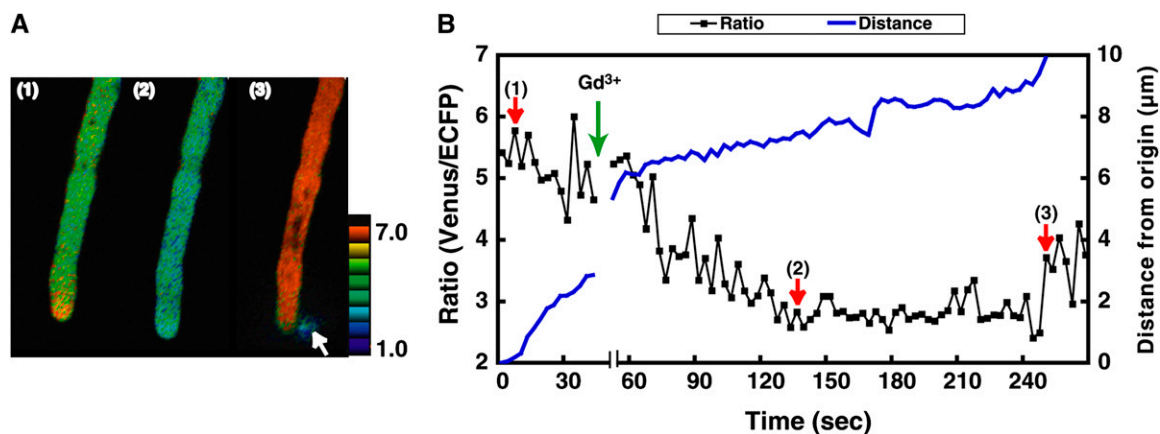
Figure 7. The effects of Gd^{3+} on the changes in the $[Ca^{2+}]_{cyt}$ in the tip region of Arabidopsis pollen tubes growing in the semi-in vivo condition. A, Ratio images of a pollen tube before and after the addition of Gd^{3+}. Numbers in each figure correspond to each point in the graph shown in B. After the addition of Gd^{3+}, the tip-focused $[Ca^{2+}]_{cyt}$ gradient disappeared and the tip region burst (white arrow in 3). B, The ratio change in the tip region before and after the addition of Gd^{3+} (a green arrow) and the elongation of the pollen tube. Red arrows (1) to (3) correlate to the ratio images in Figure 7A. Blue line indicates distance from origin.

in eight of 10 pollen tubes treated with CPA (8/10 samples). The other two burst during monitoring. On the other hand, thapsigargin, another specific inhibitor of animal SERCA-type Ca^{2+}-ATPases, did not change the $[Ca^{2+}]_{ER}$ (data not shown). In these experiments, we assumed the specificity of CPA to be ER-type Ca^{2+}-ATPases. These results suggested that the pollen tube ER contains CPA-sensitive Ca^{2+}-ATPases and that the $[Ca^{2+}]_{ER}$ is maintained at high level in the growing pollen tube. Moreover, it is likely that the ER is a Ca^{2+} store in pollen tubes and that CPA-sensitive Ca^{2+}-ATPases are required for pollen tube growth.

Ca^{2+} Imaging in *N. tabacum* Pollen Tubes

Regular $[Ca^{2+}]_{cyt}$ oscillations in the tip region were rarely observed in the growing pollen tubes of YC3.60-expressing Arabidopsis, even though we monitored $[Ca^{2+}]_{cyt}$ dynamics under three conditions: in vivo, semi-in vivo, and in vitro. Previous studies, however, have reported regular in vitro $[Ca^{2+}]_{cyt}$ oscillations in growing pollen tubes from *L. longiflorum* and *N. tabacum* (Watahiki et al., 2004). To determine whether this discrepancy was caused by differences between the species, we monitored $[Ca^{2+}]_{cyt}$ dynamics under various conditions using transgenic YC3.60-expressing *N. tabacum*. Under the in vitro condition, >90% of the pollen grains germinated with elongated pollen tubes 5 h after dissemination. We monitored growing pollen tubes that were >200 μm in length at 5-s intervals (growth rate: 4.5 ± 1.8 μm/min). $[Ca^{2+}]_{cyt}$ gradients and regular $[Ca^{2+}]_{cyt}$ oscillations were evident in three of 10 pollen tubes (3/10 samples; Fig. 10, A and B; Supplemental Video S9). In these cases, the mean value of the maximum ratio was 4.0 ± 0.2, whereas the mean value of the minimum ratio was 3.6 ± 0.2 (Fig. 10B). The mean amplitude range was

0.2 ± 0.1, and the periodicity of the $[Ca^{2+}]_{cyt}$ oscillation was long, ranging from 40 to 60 s (Fig. 10B). These observations were similar to previously reported results. However, irregular oscillations were also observed in 17 of 20 pollen tubes in monitoring at 1- to 2-s intervals (17/20 samples; Fig. 10C; Table I; Supplemental Video S10). Moreover, distinct regular oscillations were observed in three of 20 pollen tubes when growth ceased or was very slow (3/20 samples; Fig. 10D; Table I; Supplemental Video S11). In these cases, the mean value of the maximum ratio was 4.8 ± 0.4, whereas the mean value of the minimum ratio was 2.8 ± 0.2 (Fig. 10D). The mean amplitude range was large, 1.0 ± 0.1, which was significantly different from the results shown in Figure 10B, although the periodicities of the $[Ca^{2+}]_{cyt}$ oscillations were similar. These data suggested that regular oscillations were not directly related to the growth rate in *N. tabacum* or Arabidopsis.
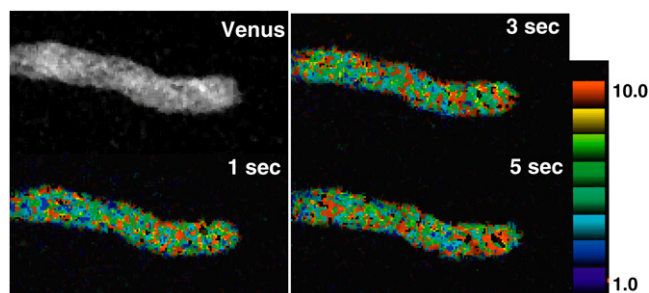

Figure 8. Imaging of the $[Ca^{2+}]_{ER}$ in Arabidopsis pollen tubes growing in the semi-in vivo condition. The YFP image shows the ER, which was localized throughout the pollen tube. In the ratio (Venus/ECFP) images of the ER, high concentration areas were scattered throughout the pollen tube.
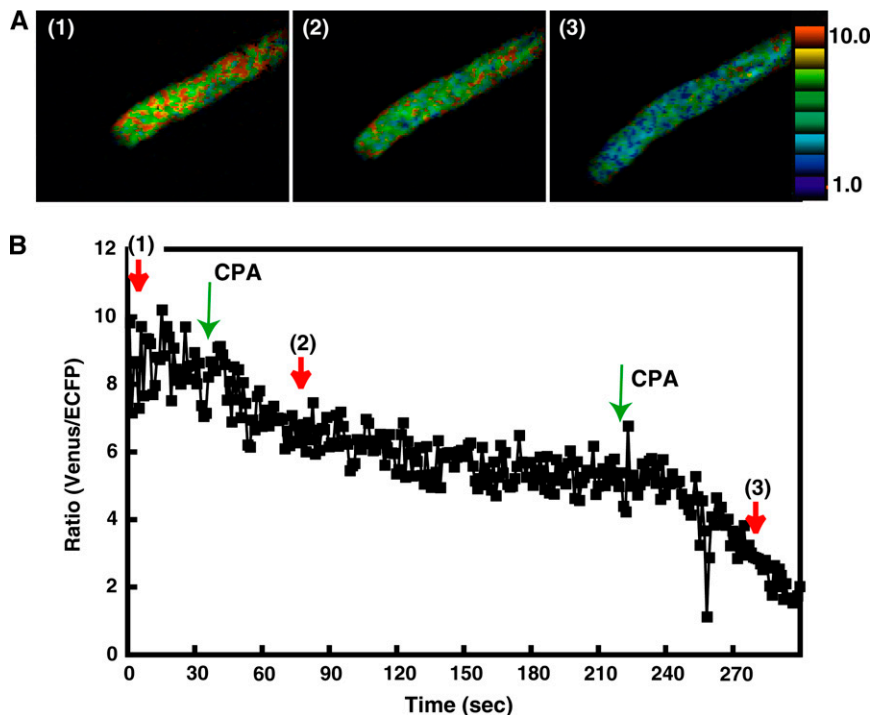
Figure 9. The effect of CPA on the [Ca^{2+}]$_{ER}$ in Arabidopsis pollen tubes growing in the semi-in vivo condition. A, Ratio images of the ER. The numbers in each figure correspond to each point in the graph shown in B. B, The ratio change in the tip region. After the addition of CPA, the ratio gradually decreased. After the addition of more CPA, the ratio decreased further.

To examine whether regular [Ca^{2+}]$_{cyt}$ oscillations occurred under the in vivo condition, we observed the stigma surface 3 h after pollination and monitored the germinated pollen tubes. Although growth was very slow in the lipophilic environment of the stigma surface, regular [Ca^{2+}]$_{cyt}$ oscillations were not observed in all experiments (15/15 samples; Fig. 11A; Table I; Supplemental Video S12). Furthermore, we monitored pollen tubes after they grew through the pistil (the semi-in vivo condition). When a pollen tube was growing well, a [Ca^{2+}]$_{cyt}$ gradient was evident but regular [Ca^{2+}]$_{cyt}$ oscillations were not observed in all experiments (30/30 samples; Fig. 11B; Table I; Supplemental Video S13). These results were not affected by the monitoring interval. Thus, regular [Ca^{2+}]$_{cyt}$ oscillations with large amplitudes were not observed in normally growing pollen tubes under three conditions: in vivo, semi-in vivo, and in vitro. These results suggested that regular [Ca^{2+}]$_{cyt}$ oscillations are not essential for pollen tube growth in *N. tabacum* or Arabidopsis.

DISCUSSION

Previously, the relationship between pollen tube growth and [Ca^{2+}]$_{cyt}$ dynamics has been examined in vitro. In this study, we monitored pollen tube growth and [Ca^{2+}]$_{cyt}$ dynamics in the pollen tubes of transgenic Arabidopsis and *N. tabacum* expressing YC3.60 using three different systems: in vitro, in vivo, and semi-in vivo. In addition, we examined the effects of inhibitors of pollen tube growth on [Ca^{2+}]$_{cyt}$ dynamics in the semi-in vivo system.

In Arabidopsis, regular oscillations were not observed under the in vivo condition, in which the pollen tube grew in the papilla cell wall. Furthermore, under the semi-in vivo condition, which is thought to mimic the in vivo condition, only irregular oscillations were observed. Finally, under the in vitro condition, irregular oscillations were observed in growing pollen tubes, whereas regular oscillations were observed only when growth stopped or was very slow. These results suggested that regular oscillations are not essential for pollen tube growth in Arabidopsis.

In *N. tabacum*, both regular and irregular [Ca^{2+}]$_{cyt}$ oscillations were observed in the tip region of normally growing pollen tubes under the in vitro condition. In addition, regular oscillations also were observed when the growth stopped or was relatively slow. Comparing the amplitudes of the regular oscillations revealed that the amplitude in slow-growing pollen tubes was 5-fold greater than that observed in normally growing pollen tubes. In the previous studies of *N. tabacum* and *L. longiflorum* transiently expressing YC2.1, regular [Ca^{2+}]$_{cyt}$ oscillations were observed in normally growing pollen tubes. The amplitude was small, however, ranging from 0.1 to 0.15 in *N. tabacum*, and the maximum ratio of the oscillation was 1.6, considerably lower than the maximum ratio of 2.7 observed after addition of the ionophore (Watahiki et al., 2004). Moreover, the amplitude was lower in *L. longiflorum* than in *N. tabacum* (Watahiki et al., 2004). Interestingly, in regular oscillations from normally growing pollen tubes, the amplitude was small in both this study and the previous study and was different from the value observed in pollen tubes that had stopped growing. Furthermore,
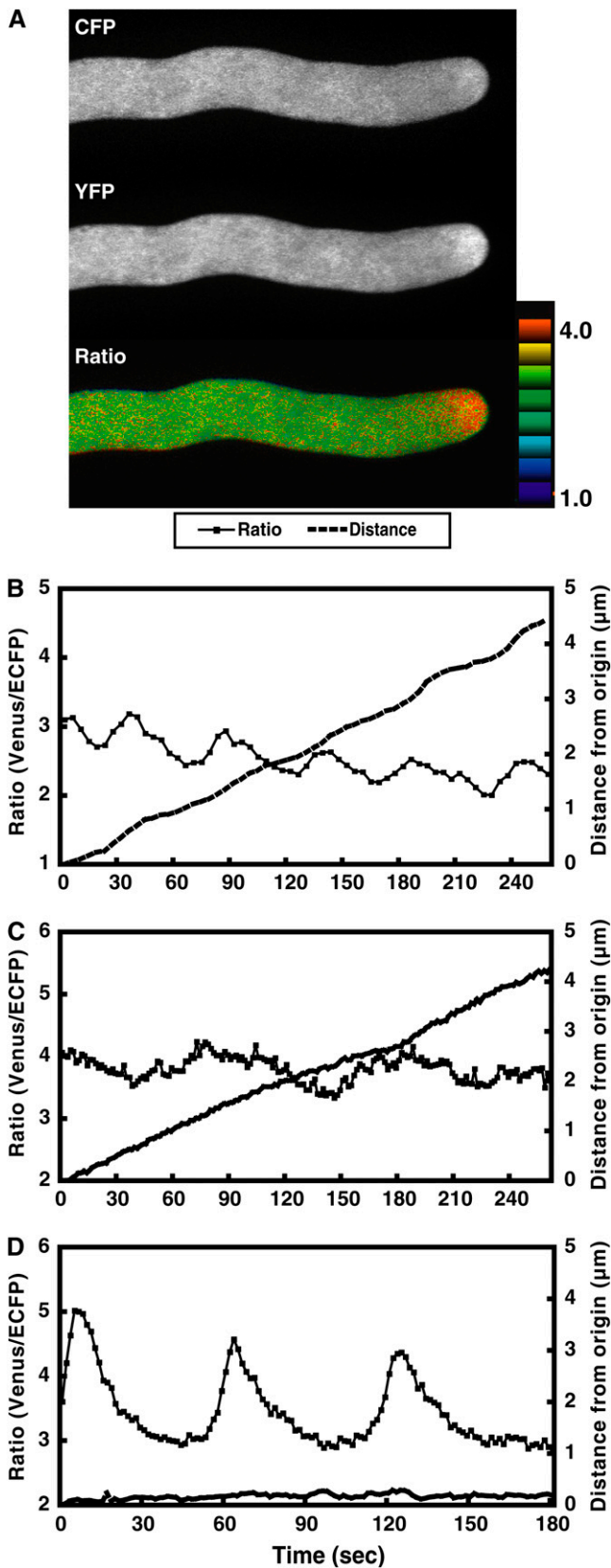
regular $[Ca^{2+}]_{cyt}$ oscillations were rarely observed in either the in vivo or semi-in vivo condition. These results suggested that regular oscillations are not essential for the pollen tube growth in *N. tabacum* as well as in Arabidopsis. $[Ca^{2+}]_{cyt}$ oscillations, which have a large amplitude range, also are not likely to be improper for pollen tube growth. In the previous experiments in *L. longiflorum*, $[Ca^{2+}]_{cyt}$ do not regularly oscillate in the short pollen tubes about 30 min after germination, while $[Ca^{2+}]_{cyt}$ regularly oscillates in the elongated pollen tubes 3 h after germination (Pierson et al., 1996; Messerli and Robinson, 1997; Feijó et al., 2001). These reports reinforced our conclusion that regular oscillations are not essential for the pollen tube growth. On the other hand, based on the data that the tip-focused $[Ca^{2+}]_{cyt}$ gradient oscillates with the same period as the growth rate (Pierson et al., 1996; Messerli et al., 2000; Holdaway-Clarke and Hepler, 2003; Messerli and Robinson, 2003), models that the growth rate and $[Ca^{2+}]_{cyt}$ were correlated have been presented (Holdaway-Clarke et al., 1997). In addition, it has been reported that the Rop GTPase activity regulating $[Ca^{2+}]_{cyt}$ influx oscillated with the same period as the growth (Li et al., 1999; Hwang et al., 2005). Although we could not examine whether regular oscillation occurs in the nongrowing pollen tube of *L. longiflorum* or whether Rop GTPase activity oscillates in Arabidopsis, our results showed cases where $[Ca^{2+}]_{cyt}$ oscillation was not correlated with the growth rate. For pollen tube growth, it is both important and essential to fine-tune the components that regulate $[Ca^{2+}]_{cyt}$. In living cells, the $[Ca^{2+}]_{cyt}$ is critical for many cellular responses and must be maintained at a level approximately 2×10^4 lower than the extracellular $[Ca^{2+}]$ (Petersen et al., 2005; Clapham 2007). In addition, $[Ca^{2+}]_{cyt}$ oscillations are thought to control a diverse range of intracellular processes, which may be regulated by the amplitude, frequency, shape, or any combination of characteristics related to the oscillations (Petersen et al., 2005). We speculate that maintaining the $[Ca^{2+}]_{cyt}$ in a narrow range is important for Ca^{2+} homeostasis in the pollen tube.

In *L. longiflorum*, $[Ca^{2+}]_{cyt}$ dynamics in pollen tubes growing in vitro has been examined, revealing that regular $[Ca^{2+}]_{cyt}$ oscillations correlated with the growth rate (Pierson et al., 1996; Messerli et al., 2000; Holdaway-Clarke and Hepler, 2003; Messerli and Robinson, 2003). Although we could not compare the in vitro $[Ca^{2+}]_{cyt}$ dynamics with those observed under

vitro condition. A, ECFP, Venus, and ratio (Venus/ECFP) images of an elongated pollen tube 5 h after dissemination. A tip-focused $[Ca^{2+}]_{cyt}$ gradient was observed. The ratio was measured in a tip area with a diameter of 8 μm. B, The ratio change in the tip region and elongation during monitoring of a normally growing pollen tube. Regular oscillations were observed but the amplitude was small. C, The ratio change in the tip region of a normally growing pollen tube and the distance moved during monitoring. The amplitude and periodicity of the oscillations were irregular. D, Regular oscillations in a pollen tube that was not growing. The amplitude was larger than that in A.
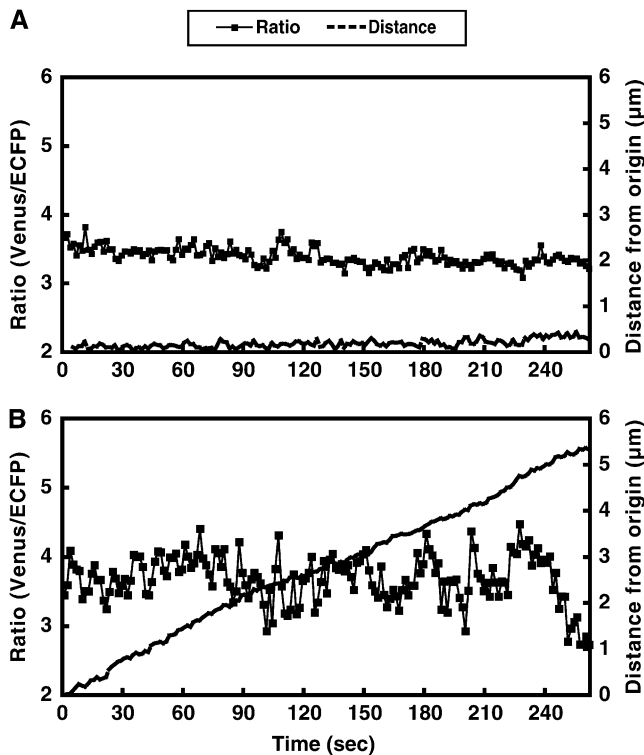
Figure 10. Regular and irregular $[Ca^{2+}]_{cyt}$ oscillations observed in elongated *N. tabacum* pollen tubes 5 h after dissemination under the in

A

B

Figure 11. Irregular oscillations observed in *N. tabacum* pollen tubes growing on the stigma (in vivo condition) and in pollen tubes growing through a style and then on germination medium (semi-in vivo condition). A, The ratio change in the tip and elongation of a pollen tube growing on a stigma. The amplitude and periodicity of the oscillations were irregular, whereas the growth rate was relatively low. B, The ratio change in growing pollen tubes under the semi-in vivo condition. The amplitude and periodicity were irregular.

the in vivo and semi-in vivo conditions, irregular oscillations may occur under the in vivo or semi-in vivo condition in *L. longiflorum* and *N. tabacum*. In fact, TTS (for transmitting tissue specific protein), which is secreted by the pistil, has been shown to attract pollen tubes and stimulate their growth in *N. tabacum* (Cheung et al., 1995). Thus, molecules released from the pistil may affect $[Ca^{2+}]_{cyt}$ dynamics in the pollen tube under in vivo or semi-in vivo conditions.

Changes in the $[Ca^{2+}]_{cyt}$ are thought to be regulated by transporters localized in Ca^{2+} stores and the plasma membrane (Sze et al., 2000). The identities of the compartments that function as Ca^{2+} stores in the pollen tube, however, were previously unknown. In this study, we visualized $[Ca^{2+}]_{ER}$ dynamics using transgenic Arabidopsis pollen expressing YC4.60, a modified fluorescent Ca^{2+} indicator with a relatively low affinity for Ca^{2+}, making it suitable for the analysis of $[Ca^{2+}]_{ER}$ dynamics against a high background $[Ca^{2+}]_{ER}$. Although the ERs were localized throughout the pollen tube, the $[Ca^{2+}]_{ER}$ was not homogeneous and areas containing a high local $[Ca^{2+}]_{ER}$ (e.g. 100–500 μM) were scattered throughout the pollen tubes. This result supports the idea that the $[Ca^{2+}]_{ER}$ is heteroge-

neous due to an uneven distribution of ER Ca^{2+}-binding proteins (Clapham, 2007). Thus, our results indicated that the ER is a Ca^{2+} store in growing pollen tubes.

Ca^{2+}-sensitive vibrating electrodes and patch-clamp electrophysiology have been used to examine Ca^{2+} influx in the tip region (Kuhtreiber and Jaffe, 1990; Pierson et al., 1994; Holdaway-Clarke et al., 1997; Franklin-Tong et al., 2002; Dutta and Robinson, 2004). In this study, we always observed a tip-focused $[Ca^{2+}]_{cyt}$ gradient in growing pollen tubes, with a submicromolar $[Ca^{2+}]_{cyt}$ in the tip region. In addition, the regions showing a high $[Ca^{2+}]_{ER}$ were scattered throughout the pollen tubes. These data suggested that Ca^{2+} imported through the plasma membrane in the tip region immediately moved into Ca^{2+} stores.

When Gd^{3+} was added to the samples, $[Ca^{2+}]_{cyt}$ at the tip region decreased and the $[Ca^{2+}]_{cyt}$ gradient disappeared from the tip region. On the other hand, just after the addition of CPA to the culture medium, the area with a high $[Ca^{2+}]_{cyt}$ increased in size. The $[Ca^{2+}]_{cyt}$ increase is thought to be the result of CPA impairing the ability to restore the cytoplasmic Ca^{2+}. After the $[Ca^{2+}]_{cyt}$ increase, $[Ca^{2+}]_{cyt}$ was decreased and then regular $[Ca^{2+}]_{cyt}$ oscillations were induced. The result that Gd^{3+} inhibited $[Ca^{2+}]_{cyt}$ oscillations suggested that an imbalance of extracellular Ca^{2+} influx and Ca^{2+} efflux to outside would induce the regular $[Ca^{2+}]_{cyt}$ oscillations.

In this study, the results that CPA decreased $[Ca^{2+}]_{ER}$ and induced $[Ca^{2+}]$ oscillations suggested that the ER contains CPA-sensitive Ca^{2+}-ATPases and that CPA affected Ca^{2+} efflux from the cytoplasm to the ER. Thapsigargin, another inhibitor of type IIA Ca^{2+}-ATPases, did not induce a decrease in the $[Ca^{2+}]_{ER}$, however. Four different IIA-type Ca^{2+}-ATPases and 10 different IIB-type Ca^{2+}-ATPases have been identified in Arabidopsis. One of the IIA-type Ca^{2+}-ATPases, ECA1, is inhibited by CPA but not thapsigargin (Liang et al., 1997; Liang and Sze, 1998; Sze et al., 2000), making it a good candidate for the CPA-sensitive Ca^{2+}-ATPase in the ER of the pollen tube. On the other hand, one of the IIB-type Ca^{2+}-ATPases, ACA2, is not inhibited by CPA, is present in ER, and is expressed in pollen grains (Harper et al., 1998; Hwang et al., 2000). As CPA at a concentration that induced $[Ca^{2+}]_{cyt}$ oscillations did not completely deplete the $[Ca^{2+}]_{ER}$ in this study, a CPA-insensitive Ca^{2+}-ATPase in the ER might be related with the $[Ca^{2+}]_{cyt}$ oscillations. In addition, ECA3, another IIA-type Ca^{2+}-ATPase from Arabidopsis, has been detected in the Golgi apparatus (Mills et al., 2008), and a CPA-sensitive Ca^{2+} pump has been identified in both ER vesicles and the Golgi apparatus of *Pisum sativum* (Ordenes et al., 2002). Furthermore, vesicle accumulation independent of the ER was observed in the pollen tip of *L. longiflorum* (Parton et al., 2003; Bove et al., 2008). In addition, there is a possibility that a CPA-sensitive Ca^{2+} pump exists in vacuolar membrane. Therefore, the induction of regular $[Ca^{2+}]_{cyt}$ oscillations by CPA may be related to Ca^{2+}-ATPases not only in the ER but also in other

intracellular compartments, such as Golgi vesicles and vacuoles.

In this study, we visualized cytoplasmic Ca^{2+} dynamics in pollen tubes growing under in vitro, in vivo, and semi-in vivo conditions in Arabidopsis and *N. tabacum* with a higher resolution, higher speed, and higher FRET efficiency compared with previously reported results from YC3.1-expressing Arabidopsis (Iwano et al., 2004). The tip-focused $[Ca^{2+}]_{cyt}$ gradient was always observed in growing pollen tubes. Regular oscillations of the $[Ca^{2+}]_{cyt}$, however, were rarely identified in Arabidopsis or *N. tabacum* pollen tubes grown under the in vivo condition or in the semi-in vivo condition. On the other hand, regular oscillations were observed in vitro in both growing and nongrowing pollen tubes, although the oscillation amplitude was 5-fold greater in the nongrowing pollen tubes compared with growing pollen tubes. Although models that the growth rate and $[Ca^{2+}]_{cyt}$ were correlated have been presented previously (Holdaway-Clarke et al., 1997), it was shown that $[Ca^{2+}]_{cyt}$ oscillation was not always correlated with the growth rate. Our results suggested that a submicromolar $[Ca^{2+}]_{cyt}$ in the tip region is essential for pollen tube growth, whereas a regular $[Ca^{2+}]$ oscillation is not. In addition, our results revealed that the ER acts as a Ca^{2+} store in pollen tubes and that CPA-sensitive Ca^{2+}-ATPases in the ER function to maintain a high $[Ca^{2+}]_{ER}$. Furthermore, CPA-sensitive Ca^{2+}-ATPases are likely required to maintain a narrow range of the $[Ca^{2+}]_{cyt}$ in growing pollen tubes.

MATERIALS AND METHODS

Plant Materials and Growth Conditions

Arabidopsis (*Arabidopsis thaliana*) ecotype Columbia was used in all of the experiments. Arabidopsis plants were grown in mixed soil in a growth chamber. The light intensity was 120 to 150 μmol m^{-2} s^{-1} during the daily 12-h light period. The temperature was maintained at 22°C ± 2°C. *Nicotiana tabacum* cv SR1 was grown in mixed soil in a greenhouse, in which the temperature was maintained at 25°C ± 2°C.

Transgenic Constructs

A cassette containing the YC3.60-coding region followed by the nopaline synthase polyadenylation signal from pBIYC3.60 was constructed by replacing the GUS-coding sequence of pBI221 (CLONTECH) with the YC3.60-coding region. The 1.5-kb fragment upstream of the *Act1* gene, which is highly expressed in reproductive tissues (An et al., 1996), was PCR amplified using the specific primers 5′-<u>GAAGCTT</u>TCTCTTTAAAAGTTAAGTTTTCTTTG-TACATGTCTCTAAGC-3′ and 5′-<u>GTCTAGA</u>TTTCTTCTACCTTTATGCA-AATCCAAACATTGTTTAAAGATC-3′ (the underlined sequences show the incorporated *Hind*III and *Xba*I sites, respectively). The amplified fragments were subcloned into pBIYC3.60 to yield Act1 promoter-YC3.60. The chimeric gene comprising the 1.5-kb promoter region of the *Act1* gene, the YC3.60 coding sequence, and the nopaline synthase transcription terminator were inserted into the binary vector pSLJ1006 (Jones et al., 1992) to create pAct1::YC3.60.

To express YC4.60 in the pollen tube ER, the DNA fragment encoding YC3.60 in pSLG9-YC3.60 was replaced with that encoding YC4.60 in pcDNA-YC4.60, which yielded pSLG9-YC4.60. To construct a vector encoding ER-targeted YC4.60, a signal peptide and ER retention signal sequence were designed according to a previous report (Mitsuhashi et al., 2000). A

double-strand oligonucleotide encoding the signal peptide (5′-GGCC-GGATCCATGGCTAGATTGACTTCTATTATTGCTTTGTTTGCTGTTGCTT-TGTTGGTTGCTGATGCTTATGCTTATCGTAC-3′ as the sense strand and 5′-CATGGTACGATAAGCATAAGCATCAGCAACCAACAAAGCAACAGC-AAACAAAGCAATAATAGAAGTCAATCTAGCCATGGATCC-3′ as the antisense strand) was synthesized and ligated into the *Eco*52I and *Nco*I sites of pSLG9::YC4.60, yielding pSLG9::SP-YC4.60. To synthesize a DNA fragment encoding the C-terminal portion of YC4.60 with an ER retention signal, a PCR was performed using specific primers (5′-AAGAAGATCTCCAGCTCCGG-GGCACTGGAGCTTAT-3′ and 5′-AATAGAGCTCACAATTCATCATGATG-ATGATGATGATGTCCACCTCCCTCGATGTTGTGGCGGATCT-3′) and pSLG9::YC4.60 as the template. The obtained fragment was digested with *Bgl*II and *Sac*I, and ligated to the *Bgl*II and *Sac*I sites of pSLG9::SP-YC4.60, yielding pSLG9::SP-YC4.60-ER.

A DNA fragment from pSLG9::SP-YC4.60-ER encoding SP-YC4.60-ER was PCR amplified using specific primers (5′-ACGGTCTAGATGGCTAGATT-GACTTCTATTATTG-3′ and 5′-AATAGAGCTCACAATTCATCATGATGAT-GATGATGATGTCCACCTCCCTCGATGTTGTGGCGGATCT-3′). The obtained DNA fragment was digested with *Xba*I and *Sac*I, and ligated into the *Xba*I and *Sac*I sites of pBI121-pAct1::YC3.60, resulting in pBI121-pAct1::YC4.60(ER).

To express YC3.60 in the *N. tabacum* pollen tube cytoplasm, the 35S promoter and GUS reporter gene in pBI121 were replaced with the microspore-specific Lat52 promoter from pBI121-pLat52::GUS (Twell et al., 1991) and the YC3.60-coding fragment from pSLG9-YC3.60, which yielded pLat52::YC3.60.

Transformation

The pSLJAct1-YC3.60 and pSLJAct1-YC4.60 plasmids were electroporated into *Agrobacterium tumefaciens* strain EHA105 (Hood et al., 1993). For Arabidopsis, the *Agrobacterium* infiltration procedure was performed with unopened flower buds of Arabidopsis ecotype Columbia as previously described (Bechtold and Pelletier, 1998). The transformed seeds were selected on half-strength Murashige and Skoog plates containing kanamycin (50 μg/mL) and were analyzed using PCRs to test for the presence of the YC3.60 gene. For *N. tabacum*, the *Agrobacterium* infiltration procedure was performed with leaf discs from *N. tabacum* cv SR1 as previously described (Horsch et al., 1985).

Pollen Tube Growth, Ratiometric Imaging, and Image Analysis

For in vitro imaging, pollen grains from freshly dehisced anthers of YC3.60-expressing plants were mounted on modified germination medium containing 2 mM $CaCl_2$, 0.01% boric acid, 1 mM $MgSO_4$, 1% (w/v) agar (ultralow gelling temperature type IX-A; Sigma-Aldrich), and 17% (w/v) Suc (pH adjusted to 7.0 using KOH) in moistened glass-bottomed dishes (Palanivelu et al., 2003) for Arabidopsis or germination medium (Read et al., 1993) containing 0.5% (w/v) agar for *N. tabacum*. After 5 h at 20°C for Arabidopsis and at 25°C for *N. tabacum*, pollen tubes that were at least 200 μm in length were imaged with an Olympus IX81 inverted microscope equipped with a CSU-22 spinning Nipkow disc confocal unit, an EM-CCD C9100 camera (Hamamatsu), an image splitter (Dual-View; Optical Insights), and a diode-pumped solid-state 445-nm laser (iFLEX2000; Point Source). Imaging of the cameleon emission ratio was accomplished using two emission filters (480/30 for ECFP and 535/40 for Venus). After a background subtraction, the Venus/ECFP ratio was determined using MetaMorph software. An Olympus UPlanSApo 60×/1.35w immersion objective lens was used for imaging. In each experiment, the ratio in a region with a diameter of 6 μm was measured using the MetaMorph software and is shown as sequential line graphs. For analysis of the changes in the $[Ca^{2+}]$, the maximum and the minimum values in each periodicity were measured, allowing calculation of the amplitude in each periodicity. In each experiment, the mean maximum, minimum, and amplitude values were calculated using Excel software. Exposure times were typically 50 to 500 ms, and images were collected every 0.5 to 5 s.

To confirm that full-length cameleon was expressed in the pollen tube, elongated pollen tubes were monitored with excitation at 458 nm using a spectral imaging fluorescence microscope system (LSM510 META; Carl Zeiss). This system is capable of resolving the spectra of various fluorescence images; therefore, we were able to obtain images with no interference from the overlapping fluorescence emissions (Haraguchi et al., 2002; Iwano et al., 2004). A Zeiss 63× W Korr objective lens (numerical aperture of 1.2) was used to image the pollen tubes.

To examine the effects of a Ca^{2+} channel blocker, Gd^{3+} (Sigma-Aldrich) was dissolved in the germination medium. To examine the effects of a P-type IIA Ca^{2+}-ATPase inhibitor, CPA was dissolved in dimethyl sulfoxide and added to the germination medium to a final concentration of 10 to 100 μM. Dimethyl sulfoxide alone had no discernible effects on germination or tube growth.

For in vivo imaging in Arabidopsis, a pistil was mounted on a coverslip prior to pollination, fixed with double-sided tape, and covered with 1% agar except for the stigma. After a pollen grain from a transgenic Arabidopsis was mounted on a wild-type Arabidopsis papilla cell using a micromanipulator, the [Ca^{2+}]$_{cyt}$ in the pollen tube growing through the papilla cell wall was monitored under dry conditions using the microscope system described above. For *N. tabacum*, the pistil was mounted on a coverslip 3 h after pollination, fixed with double-sided tape, covered with 1% agar except for the stigma, and monitored. These experiments were carried out more than 10 times.

For imaging under the semi-in vivo condition, wild-type Arabidopsis flowers excised before they dehisced were attached to an agar plate after the anthers of a transgenic Arabidopsis were removed from the flowers. Pollen grains from freshly dehisced anthers of YC3.60- or YC4.60-expressing plants were attached to the wild-type stigma. Thirty minutes after pollination, the upper half of the pollinated pistil was excised and mounted on germination medium in a moistened glass-bottomed dish. After 2 h at 20°C, the [Ca^{2+}]$_{cyt}$ in pollen tubes growing through the style was monitored using the microscope system described above. For *N. tabacum*, styles, excised before the flowers were dehisced, were attached to an agar plate and pollinated with pollen grains from freshly dehisced anthers of YC3.60-expressing plants. After 18 h at 25°C, the [Ca^{2+}]$_{cyt}$ in pollen tubes growing through the style was monitored using the microscope system described above. These experiments were carried out more than 30 times.

Calibration of YC3.60 and YC4.60 Ratiometric Changes

Calibration of the [Ca^{2+}]$_{cyt}$ was carried out as described previously (Allen et al., 1999). Serial dilutions of purified YC3.60 and YC4.60 were made in Ca^{2+} calibration buffer (Molecular Probes), in which the free [Ca^{2+}] ranged from 0 μM to 1 mM. Dilutions of YC3.60 and YC4.60 that resulted in similar signal intensities to those seen in YC3.60- and YC4.60-expressing pollen tubes were used to determine R_{min} and R_{max}. R_{min} and R_{max} values were 2.95 and 8.33 for YC3.60, and 3.53 and 9.87 for YC4.60, respectively. These values were used to convert the YC3.60 and YC4.60 fluorescence ratios into a [Ca^{2+}]$_{cyt}$ by fitting them to YC3.60 and YC4.60 calibration curves obtained in vitro.

Pollen Tube Growth Rate

The growth rate, calculated from the elongation length during a 3-min period, was obtained using Venus fluorescence in the growing pollen tube and MetaMorph software.

Statistical Analysis

Statistical analyses were performed using Student's t tests, when necessary.

Supplemental Data

The following materials are available in the online version of this article.

Supplemental Video S1. Irregular [Ca^{2+}]$_{cyt}$ oscillations in a normally growing Arabidopsis pollen tube under the in vitro condition.

Supplemental Video S2. Regular [Ca^{2+}]$_{cyt}$ oscillations in a slowly growing Arabidopsis pollen tube under the in vitro condition.

Supplemental Video S3. Regular oscillations followed by irregular oscillations in an elongated Arabidopsis pollen tube under the in vitro condition.

Supplemental Video S4. Irregular oscillations observed in an Arabidopsis pollen tube growing through a papilla cell wall (in vivo condition).

Supplemental Video S5. Irregular oscillations observed in an Arabidopsis pollen tube growing through a style and then on germination medium (semi-in vivo condition).

Supplemental Video S6. The effects of CPA and Gd^{3+} on the changes in the [Ca^{2+}]$_{cyt}$ in the tip region of Arabidopsis pollen tubes growing in the semi-in vivo condition.

Supplemental Video S7. The effects of Gd^{3+} on the changes in the [Ca^{2+}]$_{cyt}$ in the tip region of an Arabidopsis pollen tube growing in the semi-in vivo condition.

Supplemental Video S8. Imaging of the [Ca^{2+}]$_{ER}$ in an Arabidopsis pollen tube growing in the semi-in vivo condition.

Supplemental Video S9. Regular [Ca^{2+}]$_{cyt}$ oscillations observed in an elongated *N. tabacum* pollen tube.

Supplemental Video S10. Irregular [Ca^{2+}]$_{cyt}$ oscillations observed in an elongated *N. tabacum* pollen tube.

Supplemental Video S11. Regular [Ca^{2+}]$_{cyt}$ oscillations observed in a stopping *N. tabacum* pollen tube.

Supplemental Video S12. Irregular oscillations observed in a *N. tabacum* pollen tube growing on the stigma (in vivo condition).

Supplemental Video S13. Irregular oscillations observed in a *N. tabacum* pollen tube growing through a style and then on germination medium (semi-in vivo condition).

LITERATURE CITED

Allen GJ, Chu SP, Harrington CL, Schumacher K, Hoffman T, Tang YY, Grill E, Schroeder JI (2001) A defined range of guard cell calcium oscillation parameters encodes stomatal movements. Nature **411:** 1053–1057

Allen GJ, Chu SP, Schumacher K, Shimazaki CT, Vafeados D, Kemper A, Hawke SD, Tallman G, Tsien RY, Harper JF, et al (2000) Alteration of stimulus-specific guard cell calcium oscillations and stomatal closing in Arabidopsis det3 mutant. Science **289:** 2338–2342

Allen GJ, Kwak JM, Chu SP, Llopis J, Tsien RY, Harper JF, Schroeder JI (1999) Cameleon calcium indicator reports cytoplasmic calcium dynamics in Arabidopsis guard cells. Plant J **19:** 735–747

An YQ, Huang S, McDowell JM, McKinney EC, Meagher RB (1996) Conserved expression of the *Arabidopsis* ACT1 and ACT3 actin subclass in organ primordia and mature pollen. Plant Cell **8:** 15–30

Bechtold N, Pelletier G (1998) In planta Agrobacterium-mediated transformation of adult Arabidopsis thaliana plants by vacuum infiltration. Methods Mol Biol **82:** 259–266

Bove J, Vaillancourt B, Kroeger J, Hepler PK, Wiseman PW, Geitmann A (2008) Magnitude and direction of vesicle dynamics in growing pollen tubes using spatiotemporal image correlation spectroscopy and fluorescence recovery after photobleaching. Plant Physiol **147:** 1646–1658

Brewbaker JL, Kwack BH (1963) The essential role of calcium ion in pollen germination and pollen tube growth. Am J Bot **50:** 859–865

Cheung AY, Wang H, Wu HM (1995) A floral transmitting tissue-specific glycoprotein attracts pollen tubes and stimulates their growth. Cell **82:** 383–393

Cheung AY, Wu HM (2008) Structural and signaling networks for the polar cell growth machinery in pollen tubes. Annu Rev Plant Biol **59:** 547–572

Clapham DE (2007) Calcium signaling. Cell **131:** 1047–1058

Dutta R, Robinson KR (2004) Identification and characterization of stretch-activated ion channels in pollen protoplasts. Plant Physiol **135:** 1398–1406

Feijó JA, Sainhas J, Holdaway-Clarke T, Cordeiro MS, Kunkel JG, Hepler PK (2001) Cellular oscillations and the regulation of growth: the pollen tube paradigm. Bioessays **23:** 86–94

Franklin-Tong VE, Holdaway-Clarke TL, Straatman KR, Kunkel JG, Hepler PK (2002) Involvement of extracellular calcium influx in the self-incompatibility response of *Papaver rhoeas*. Plant J **29:** 333–345

Frietsch S, Wang YF, Sladek C, Poulsen LR, Romanowsky SM, Schroeder

JI (2007) A cyclic nucleotide-gated channel is essential for polarized tip growth of pollen. Proc Natl Acad Sci USA **104**: 14531–14536

Geisler M, Axelsen KB, Harper JF, Palmgren MG (2000) Molecular aspects of higher plant P-type Ca^{2+}-ATPases. Biochim Biophys Acta **1465**: 52–78

Geitmann A, Cresti M (1998) Ca^{2+} channels control the rapid expansions in pulsating growth of *Petunia hybrida* pollen tubes. J Plant Physiol **152**: 439–447

Haraguchi T, Shimi T, Koujin T, Hashiguchi N, Hiraoka Y (2002) Spectral imaging fluorescence microscopy. Genes Cells **7**: 881–887

Harper JF, Hong B, Hwang I, Guo HQ, Stoddard R, Huang JF, Palmgren MG, Sze H (1998) A novel calmodulin-regulated Ca^{2+}-ATPase (ACA2) from Arabidopsis with an N-terminal autoinhibitory domain. J Biol Chem **273**: 1099–1106

Holdaway-Clarke TL, Feijo JA, Hackett GR, Kunkel JG, Hepler PK (1997) Pollen tube growth and the intracellular cytosolic calcium gradient oscillate in phase while extracellular calcium influx is delayed. Plant Cell **9**: 1999–2010

Holdaway-Clarke T, Hepler P (2003) Control of pollen tube growth: role of ion gradients and fluxes. New Phytol **159**: 539–563

Hood EE, Gelvin SB, Melchers LS, Hoekema A (1993) New agrobacterium helper plasmids for gene transfer to plants. Transgenic Res **2**: 208–218

Horsch RB, Fry JE, Hoffmann NL, Eichholtz D, Rogers SG, Fraley RT (1985) A simple and general method for transferring genes into plants. Science **227**: 1229–1231

Hwang I, Sze H, Harper JF (2000) A calcium-dependent protein kinase can inhibit a calmodulin-stimulated Ca^{2+} pump (ACA2) located in the endoplasmic reticulum of *Arabidopsis*. Proc Natl Acad Sci USA **97**: 6224–6229

Hwang JU, Gu Y, Lee YJ, Yang Z (2005) Oscillatory ROP GTPase activation leads the oscillatory polarized growth of pollen tubes. Mol Biol Cell **16**: 5385–5399

Inesi G, Sagara Y (1994) Specific inhibitors of intracellular Ca^{2+} transport ATPases. J Membr Biol **141**: 1–6

Iwano M, Shiba H, Miwa T, Che FS, Takayama S, Nagai T, Miyawaki A, Isogai A (2004) Ca^{2+} dynamics in a pollen grain and papilla cell during pollination of Arabidopsis. Plant Physiol **136**: 3562–3571

Jones JDG, Shlumukov L, Carland F, English J, Scofield SR, Bishop GJ, Harrison K (1992) Effective vectors for transformation, expression of heterologous genes, and assaying transposon excision in transgenic plants. Transgenic Res **1**: 285–297

Kuhtreiber WM, Jaffe LF (1990) Detection of extracellular calcium gradients with a calcium-specific vibrating electrode. J Cell Biol **110**: 1565–1573

Li H, Lin Y, Heath RM, Zhu MX, Yang Z (1999) Control of pollen tube tip growth by a Rop GTPase-dependent pathway that leads to tip-localized calcium influx. Plant Cell **11**: 1731–1742

Liang F, Cunningham KW, Harper JF, Sze H (1997) ECA1 complements yeast mutants defective in Ca^{2+} pumps and encodes an endoplasmic reticulum-type Ca^{2+}-ATPase in *Arabidopsis thaliana*. Proc Natl Acad Sci USA **94**: 8579–8584

Liang F, Sze H (1998) A high-affinity Ca^{2+} pump, ECA1, from the endoplasmic reticulum is inhibited by cyclopiazonic acid but not by thapsigargin. Plant Physiol **118**: 817–825

Malhó R, Read ND, Pais MS, Trewavas AJ (1994) Role of cytosolic free alcium in the reorientation of pollen tube growth. Plant J **5**: 331–341

Messerli MA, Creton R, Jaffe LF, Robinson KR (2000) Periodic increases in elongation rate precede increases in cytosolic Ca^{2+} during pollen tube growth. Dev Cell **222**: 84–98

Messerli M, Robinson KR (1997) Tip localized Ca^{2+} pulses are coincident with peak pulsatile growth rates in pollen tubes of *Lilium longiflorum*. J Cell Sci **110**: 1269–1278

Messerli MA, Robinson KR (2003) Ionic and osmotic disruptions of the lily pollen tube oscillator: testing proposed models. Planta **217**: 147–157

Mills RF, Doherty ML, Lopez-Marques RL, Weimar T, Dupree P, Palmgren MG, Pittman JK, Williams LE (2008) ECA3, a Golgi-localized P2A-type ATPase, plays a crucial role in manganese nutrition in Arabidopsis. Plant Physiol **146**: 116–128

Mitsuhashi N, Shimada T, Mano S, Nishimura M, Hara-Nishimura I (2000) Characterization of organelles in the vacuolar-sorting pathway by visualization with GFP in tobacco BY-2 cells. Plant Cell Physiol **41**: 993–1001

Miyawaki A, Llopis J, Heim R, McCaffery JM, Adams JA, Ikura M, Tsien RY (1997) Fluorescent indicators for Ca^{2+} based on green fluorescent proteins and calmodulin. Nature **388**: 834–835

Miwa H, Sun J, Oldroyd GE, Downie JA (2006) Analysis of calcium spiking using a cameleon calcium sensor reveals that nodulation gene expression is regulated by calcium spike number and the developmental status of the cell. Plant J **48**: 883–894

Nagai T, Ibata K, Park ES, Kubota M, Mikoshiba K, Miyawaki A (2002) A variant of yellow fluorescent protein with fast and efficient maturation for cell-biological applications. Nat Biotechnol **20**: 87–90

Nagai T, Yamada S, Tominaga T, Ichikawa M, Miyawaki A (2004) Expanded dynamic range of fluorescent indicators for Ca^{2+} by circularly permuted yellow fluorescent proteins. Proc Natl Acad Sci USA **101**: 10554–10559

Ordenes VR, Reyes FC, Wolff D, Orellana A (2002) A thapsigargin-sensitive Ca^{2+} pump is present in the pea Golgi apparatus membrane. Plant Physiol **129**: 1820–1828

Palanivelu R, Brass L, Edlund AF, Preuss D (2003) Pollen tube growth and guidance is regulated by POP2, an Arabidopsis gene that controls GABA levels. Cell **114**: 47–59

Parton RM, Fischer-Parton S, Trewavas AJ, Watahiki MK (2003) Pollen tubes exhibit regular periodic membrane trafficking events in the absence of apical extension. J Cell Sci **116**: 2707–2719

Petersen OH, Michalak M, Verkhratsky A (2005) Calcium signaling: past, present and future. Cell Calcium **38**: 161–169

Pierson ES, Miller DD, Callaham DA, Shipley AM, Rivers BA, Cresti M, Hepler PK (1994) Pollen tube growth is coupled to the extracellular calcium ion flux and the intracellular calcium gradient: effect of BAPTA-type buffers and hypertonic media. Plant Cell **6**: 1815–1828

Pierson ES, Miller DD, Callaham DA, van Aken J, Hackett G, Hepler PK (1996) Tip-localized calcium entry fluctuates during pollen tube growth. Dev Biol **174**: 160–173

Read SM, Clarke AE, Bacic A (1993) Stimulation of growth of cultured *Nicotiana tabacum* W 38 pollen tubes by poly(ethylene glycol) and $Cu_{(II)}$ salts. Protoplasma **177**: 1–14

Sze H, Liang F, Hwang I (2000) Diversity and regulation of plant Ca^{2+} pumps: insights from expression in yeast. Annu Rev Plant Physiol Plant Mol Biol **51**: 433–462

Twell D, Yamaguchi J, Wing RA, Ushiba J, Mccormick S (1991) Promoter analysis of genes that are coordinately expressed during pollen development reveals pollen-specific enhancer sequences and shared regulatory elements. Genes Dev **5**: 496–507

Watahiki MK, Trewavas AJ, Parton RM (2004) Fluctuations in the pollen tube tip-focused calcium gradient are not reflected in nuclear calcium level: a comparative analysis using recombinant yellow cameleon calcium reporter. Sex Plant Reprod **17**: 125–130